

# Detection of Unknown-Unknowns in Cyber-Physical Systems using Statistical Conformance with Physics Guided Process Models

Aranyak Maity

*Impact Lab*

*Arizona State University*

Tempe, USA

amaity1@asu.edu

Ayan Banerjee

*Impact Lab*

*Arizona State University*

Tempe, USA

abanerj3@asu.edu

Sandeep K.S. Gupta

*Impact Lab*

*Arizona State University*

Tempe, USA

sandeep.gupta@asu.edu

**Abstract**—Unknown unknowns are operational scenarios in a cyber-physical system that are not accounted for in the design and test phase. As such under unknown-unknown scenarios, the operational behavior of the CPS is not guaranteed to meet requirements such as safety and efficacy specified using Signal Temporal Logic (STL) on the output trajectories. We propose a novel framework for analyzing the stochastic conformance of operational output characteristics of safety-critical cyber-physical systems that can discover unknown-unknown scenarios and evaluate potential safety hazards. We propose dynamics-induced hybrid recurrent neural networks (DiH-RNN) to mine a physics-guided surrogate model (PGSM) which is used to check the model conformance using STL on the model coefficients. We demonstrate the detection of operational changes in an Artificial Pancreas(AP) due to unknown insulin cartridge errors.

**Index Terms**—Operational Data Conformance Testing, Physics Guided Model Mining, Cyber-Physical Systems, Fault Detection

## I. INTRODUCTION

Safety critical human-in-the-plant (HIP) applications such as Artificial Pancreas (AP) [15] and Semi-Autonomous Driving (SAD) [10] operate in a human-in-the-loop (HIL) paradigm, where the artificial intelligence (AI) enabled autonomous system (AAS) operates with full autonomy under most input conditions while provisioning for manual override in case of potential catastrophic safety or efficacy loss [10]. Full-scale modeling of context-dependent HIL interaction with the AAS integrated with complex HIP dynamics may quickly lead to state explosion. Hence, in practice, there are several un-modeled components. These un-modeled components can result in unknown unknowns (U2s) in safety-certified AAS with potentially fatal consequences. This paper enables early detection of U2s and avoids any safety violations.

1) *Drawbacks of controller design approaches*: Broadly, two HIL-HIP AAS design approaches exist: a) optimal control for satisfying both efficacy and safety goals using techniques such as supervised data driven learning [4], and b) human-in-the-loop (HIL) controller synthesis [10]. In the first approach, the learning system simultaneously learns control action and control lyapunov barrier functions (CLBF), which act as a safety certificate [4]. This class of approaches consider the system

as control affine and human inputs as external perturbations within a distribution. While such approaches work well for full automation, in HIL-HIP safety critical AAS, human inputs in operational deployment bear a causal relationship with observations of both short and long term safety and efficacy and hence may not be captured merely by a stochastic process. HIL controller synthesis approach has focused on optimal / model predictive / reinforcement learning based control that incorporates a model of human action in the control design and decides on optimal switching between the AI controller and the human inputs [10]. The human user in safety-critical AAS, are in-frequently advised by agents (endocrinologists for AP or the car manufacturers and national transportation safety board in SAD) about context-dependent personalized actions to optimize efficacy and avoid safety hazards. However, in HIL-HIP safety critical AAS [9], the perception of impending safety hazards can cause the human user to apply such actions out of context. As such modeling human action is complex, resulting in un-modelled scenarios in HIL controller synthesis approach. This is one of the main causes of “unknown unknowns” (U2) in AAS safety in the operational field.

2) *Types of U2s and their aggregate effects*: In this paper, we restrict the U2s to encompass: a) un-modelled human actions, where the user of the AAS provides an input that is not certified safe during test time. b) latent sensor/ actuator errors, where a system component such as a sensor or an actuator. As a result, despite significant advances in safety engineering, AAS often fails with fatal consequences. Some failures are *unintentional*, highlighted in recent crash reports from Tesla [1], [12], lawsuit on Medtronic for their automated insulin delivery (AID) system causing 1 death and 20,000 injuries [7], and some are *intentional*, Volkswagen cheating case [3], [11]. The fault signatures are also unknown and hence can be misconstrued by the user as an efficacy loss to be mitigated by the advisory agent-guided personalization action. However, in reality, such personalization action can combine with the latent fault signature to result in fatal hazards. Insulin cartridge error in AP (or AID) was one such error, that stunted insulin delivery with no signature in the pump logs. The user

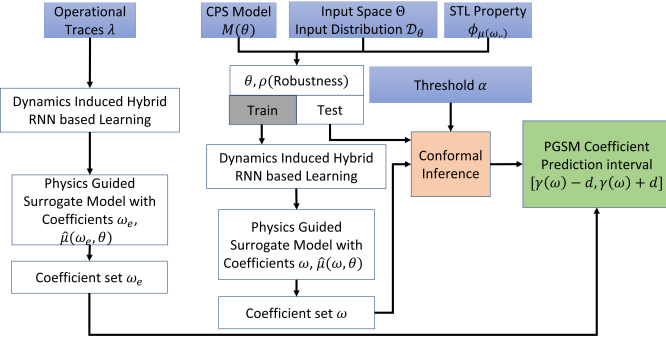
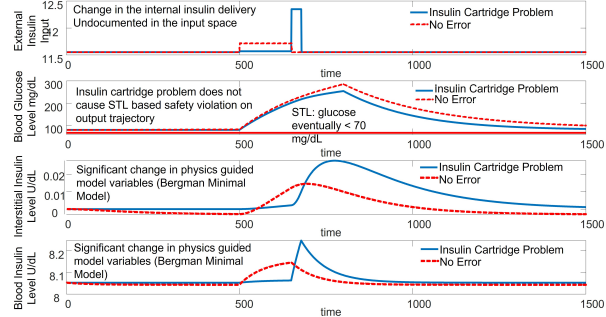


Fig. 1. Overview of the Proposed Approach based on [13].



would only perceive that the insulin delivery by the pump is not controlling a high glucose excursion. The user would follow the advisory agent-approved personalization action of administering a correction bolus either through the normal pump operational mechanism or by subverting it, a phenomenon called a phantom meal. In reality, the insulin stacking effect is induced, which eventually resulted in an unprecedented amount of insulin being delivered in a very short time, inducing severe hypoglycemia [7]. Figure 3 illustrates such a scenario. In this paper, we advocate for combining model conformance with continuous model learning to detect deviations of the sensor values from their logical combinations that follow the physics laws of the HIP. We show that unknown component errors may not have a significant effect on the actual sensor values but may drastically compromise physics laws guiding their inter-relationships.

### A. Contributions

In this paper, we make the following contributions:

- Provide a mechanism to mine physics-guided operational models from operational traces of such systems.
- Use physics-guided surrogate models to identify changes in operational characteristics due to unknown errors.
- Show a use case on detection of insulin cartridge problem in Artificial Pancreas.

### B. Advantages

The main advantage of this work over the prior STL-based stochastic verification work [13] is as follows:

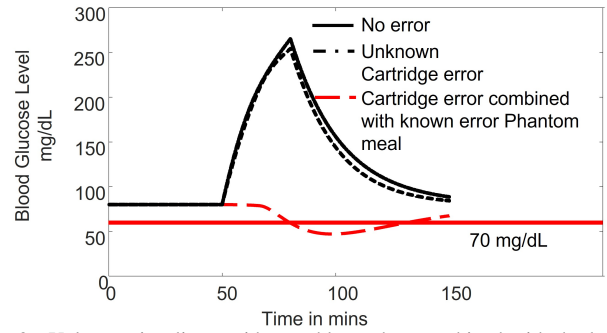


Fig. 3. Unknown insulin cartridge problem when combined with the known fault of phantom meal violates STL properties for the same input space.

- Instead of verification we perform model conformance, which enables our approach to detect unknown errors.
- We utilize physics-guided surrogate models that ensures that surrogate models learn essential internal processes of the dynamical system. As a result, it allows our technique to detect faults that are invisible in a black box model.

## II. PRELIMINARIES

**Definition 1. Trajectory and Models:** A trajectory  $\zeta$  is a function from a set  $[0, T]$  for some  $T \in \mathbb{R}^{>0}$  denoting time to a compact set of values  $\in \mathcal{R}$ . The value of a trajectory at time  $t$  is denoted as  $\zeta(t)$ . Each trajectory is the output of a CPS model  $M$ . A model  $M$  is a function that maps a  $k$  dimensional input  $\theta$  from the input space  $\Theta \subset \mathbb{R}^k$  to an output trajectory  $\zeta_\theta$ .

The input  $\theta \in \Theta$  is a random variable that follows a distribution  $\mathcal{D}_\theta$ . We also assume that for the model  $M$ , there is a simulator  $\Sigma$ . The simulator  $\Sigma$  takes the input  $\theta$  and a finite sequence of time  $t_0 \dots t_n$  with  $n$  time steps and generates the trajectory  $\zeta_\theta$  such that  $\zeta_\theta(t_i) = \Sigma(\theta, t_i)$ .

**Definition 2. Physics Model:** A physics model is a dynamical system expressed using a system of linear time-invariant ordinary differential equations in Equation 1. The system has  $n$  variables  $x_i$ ,  $i \in \{1 \dots n\}$  arranged in an  $n \times 1$  vector  $\mathcal{X}$ ,  $\mathcal{A}$  is an  $n \times n$  matrices of coefficients,  $\mathcal{B}$  is an  $n \times n$  diagonal matrix of coefficients.

$$\frac{dX(t)}{dt} = \mathcal{A}X(t) + \mathcal{B}U(t), \quad (1)$$

$$Y(t) = \beta X(t)$$

where  $U(t)$  is a  $n \times 1$  vector of external inputs.  $Y(t)$  is the  $n \times 1$  output vector of the system of equations. An  $n \times n$  diagonal matrix,  $\beta$  of 1s and 0s, where  $\beta_{ii} = 1$  indicates that the variable  $x_i$  is an observable output else it is hidden and is not available for sensing.

A formal object  $\hat{\mu}$  is a physics model when the set of models  $\mu$  can be described using the coefficient  $\omega = \mathcal{A} \cup \mathcal{B}$ . The formal object can then take any  $\theta$  as input and given the model coefficients  $\omega$ , generate a trace  $\zeta_\theta = \hat{\mu}(\omega, \theta)$ .

**Definition 3. Trace:** Concatenation of  $p$  output trajectories over time  $\zeta_{\theta_1} \zeta_{\theta_2} \dots \zeta_{\theta_p}$  is a trace  $\mathcal{T}$ .

**Definition 4.** *Continuous model mining: Given a trace  $\mathcal{T}$ , continuous model mining maps the trace into a sequence  $\Omega$  of  $p, \omega_i$ s such that  $\forall i \text{ dist}(\hat{\mu}(\omega_i, \theta_i), \zeta_{\theta_i}) < v$ , where  $\text{dist}(\cdot)$  is a distance metric between trajectories and  $v$  is a small value decided by the user.*

### A. Signal Temporal Logic

Signal temporal logic is formulas defined over trace  $\mathcal{T}$  of the form  $f(\Omega) \geq c$  or  $f(\Omega) \leq c$ . Here  $f : \mathcal{R}^p \rightarrow \mathcal{R}$  is a real-valued function and  $c \in \mathcal{R}$ . STL supports operations as shown in Equation 2.

$$\phi, \psi := \text{true} | f(\Omega) \geq c | f(\Omega) \leq c | \neg\phi | \phi \wedge \psi | \phi \vee \psi | F_I \phi | G_I \phi | \phi U_I \psi, \quad (2)$$

where  $I$  is a time interval, and  $F_I$ ,  $G_I$ , and  $U_I$  are eventually, globally, and until operations and are used according to the standard definitions [5] [6]. To compute a degree of satisfaction of the STL we consider the robustness metric.

**Definition 5.** *The robustness value  $\rho$  maps an STL  $\phi$ , the trajectory  $\zeta$ , and a time  $t \in [0, T]$  to a real value. An example robustness  $\rho$  for the STL  $\phi : f(\Omega) \geq c$  is  $\rho(f(\Omega) \geq c, \Omega, t) = f(\Omega(t)) - c$ .*

In the next section, we discuss how such a  $\delta$  surrogate model can be mined from the output trajectory of a CPS model  $M$ .

### III. LEARNING A PHYSICS-DRIVEN SURROGATE MODEL

A surrogate model is a quantitative abstraction of the black box CPS model  $M$ . A quantitative abstraction satisfies a given property on the output trajectory of the CPS model. In this paper, this quantitative property is the robustness value of an STL property. With this setting, we define a  $\delta$ -surrogate model  $\hat{\mu}$ .

**Definition 6.**  *$\delta$  surrogate model: Let  $\zeta_\theta$  be a trajectory obtained by simulating  $M$  with input  $\theta$ . Let  $\omega^T$  be the coefficients of the physics-guided representation of the original model. The model  $\hat{\mu}(\omega, \theta)$  is a  $\delta$  distance preserving quantitative abstraction if*

$$\exists \delta : \forall \theta \in \Theta : |\rho(\phi, \omega^T) - \rho(\phi, \omega)| \leq \delta \quad (3)$$

A  $\delta$  surrogate model guarantees that the robustness value evaluated on a physics model coefficient  $\omega$  derived from the trajectory  $\zeta_\theta$  will not be more than  $\delta$  away from the robustness computed on the coefficients of the original CPS model  $M$ . Obtaining such a model for arbitrary  $\delta$  is a hard problem. Hence, we define a stochastic relaxation of  $(\delta, \epsilon)$  - surrogate model.

**Definition 7.**  *$(\delta, \epsilon)$ -probabilistic surrogate model: Given a user specified  $\epsilon$ , a formal object  $\hat{\mu}$  is  $(\delta, \epsilon)$ -probabilistic surrogate model if:*

$$\exists \delta \in \mathcal{R}, \epsilon \in [0, 1] : P(|\rho(\phi, \omega^T) - \rho(\phi, \omega)| \leq \delta) \geq 1 - \epsilon. \quad (4)$$

### IV. COEFFICIENT MINING FROM TRAJECTORY

**Problem Definition 1.** *Given a set of variables  $\mathcal{X}(t)$ , a set of inputs  $U(t)$ , a  $\beta$  vector indicating observability, and a set  $\mathcal{T}$  of traces such that  $\forall i : \beta_i = 1 \exists T(x_i) \in \mathcal{T}$  and  $\forall u_j(t) \in U(t) \exists T(u_j) \in \mathcal{T}$ .*

**Derive:** approximate coefficients  $\mathcal{A}^a$  and  $\mathcal{B}^a$  such that:

- $\forall i, j | \mathcal{A}^a(i, j) - \mathcal{A}(i, j) | < \xi$
- $\forall i | \mathcal{B}^a(i, i) - \mathcal{B}(i, i) | < \xi$
- Let  $\mathcal{T}^a$  be the set of traces that include variables derived from the solution to differential equation  $\frac{dX(t)}{dt} = \mathcal{A}^a X(t) + \mathcal{B}^a U(t)$  then  $\forall i : \theta_i = 1$ , and  $\forall k \in \{1 \dots N\}, |T^a(x_i)[k] - T(x_i)[k]| < \Psi T(x_i)[k]$ ,

where  $\xi$  is the error in the coefficient estimator, while  $\Psi$  is the error factor for replicating the traces of variables with the estimated coefficients.

### A. Dynamics Induced RNN

For each variable  $x_i \in X$  the system of dynamical equations takes the form in Equation 5.

$$\frac{dx_i}{dt} = \sum_{j=1}^n a_{ij} x_j + b_{ii} u_i. \quad (5)$$

We explain Algorithm 1 using the linearized Bergman Minimal

---

#### Algorithm 1 RNN induction algorithm

---

- 1:  $\forall x_i \in X$  create an RNN node with  $n + 1$  inputs and  $x_i$  as the hidden output.
- 2: **for** each RNN node corresponding to  $x_i$  **do**
- 3:   **for** each  $j \in 1 \dots n$  **do**
- 4:     **if**  $a_{ij} \neq 0$  **then**
- 5:       Add a connection from the output of RNN node for  $x_j$  to the input of RNN node for  $x_i$ .
- 6:     **end if**
- 7:   **end for**
- 8:   Remove all other inputs in the RNN which does not have any connection.
- 9:   **for**  $e$  **do** **each**  $j \in 1 \dots n$
- 10:     **if**  $b_{ij} \neq 0$  **then**
- 11:       Add  $u_j$  as an external input to the RNN node for  $x_i$ .
- 12:     **end if**
- 13:   **end for**
- 14: **end for**
- 15: Assign arbitrary weights to each link.

---

Model (BMM) as an example. The model is a dynamical system that mimics the glucose-insulin biochemical dynamics in the human body. The Bergman Minimal model is linearized using Taylor Series expansion starting from overnight glucose dynamics and going up to time  $N$ . The linearized model is represented in Equation 6, 7 and 8.

$$\frac{d\delta i(t)}{dt} = -n\delta i(t) + p_4 u_1(t) \quad (6)$$

$$\frac{d\delta i_s(t)}{dt} = -p_1 \delta i_s(t) + p_2 (\delta i(t) - i_b) \quad (7)$$

$$\frac{d\delta G(t)}{dt} = -\delta i_s(t) G_b - p_3 (\delta G(t)) + u_2(t) / VoI, \quad (8)$$

The input vector  $U(t)$  consists of the overnight basal insulin level  $i_{1b}$  and the glucose appearance rate in the body  $u_2$ . The

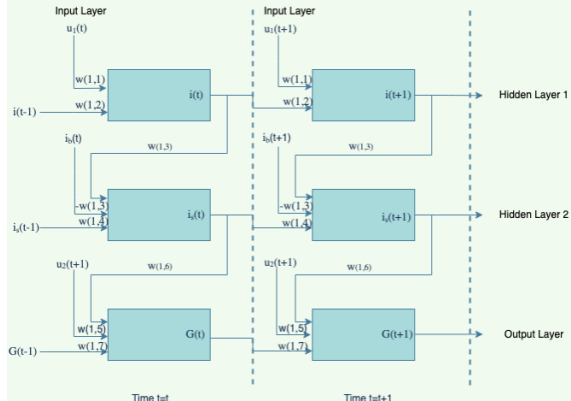


Fig. 4. DiHRNN structure of the Bergman Minimal Model.

output vector  $Y(t)$  comprises the blood insulin level  $i$ , the interstitial insulin level  $i_s$ , and the blood glucose level  $G$ . For this example, we consider that only the blood glucose level  $G$  is an observable output of the system of equations.  $i_s$  and  $i$  are intermediate outputs that are not measurable for the system of equations and only contribute to the final glucose output.  $p_1, p_2, p_3, p_4, n$ , and  $1/V_o I$  are all the coefficients of the set of differential equations. The resulting DiHRNN for the AP using Algorithm 1 is shown in figure 4

#### B. Forward pass in DiH-RNN

We prove that the Forward pass on an RNN cell estimates the solution of Eqn. 1 with error factor  $\Psi$  if  $\tau \leq \min_i \frac{\sqrt{2\Psi}}{a_{ii}}$ . Forward pass is solved for step inputs using z transforms, followed by algebraic modification and subsequent inverse z transform. Eqn. 1 is solved using Laplace transform. Equivalence under the above-mentioned restriction in sampling interval is established through limiting approximations.

#### C. Backpropagation to learn coefficients

The main aim of backpropagation is to derive the approximate coefficient matrices  $\mathcal{A}^a$  and  $\mathcal{B}^a$ . Given an error ratio of  $\phi$ , we have established that the forward pass is convergent and estimation error is proportional to  $\phi$  if  $\tau \leq \frac{\sqrt{2\Psi}}{|a_{ii}|} \forall i$ . However, we do not know  $a_{ii}$  and hence setting  $\tau$  is a difficult task. Often  $\tau$  is limited by the sampling frequency of the sensor. In this paper, we assume that the  $\tau$  satisfies the condition for convergence of the forward pass. Proposition 1 in [16] shows that for shallow DNNs if all the weights are nonnegative and the activation function is convex and non-decreasing then the overall loss is convex. In a scenario, with only a single minima the gradient descent mechanism is guaranteed to find it.

#### V. CONFORMAL INFERENCE

Conformal inference [8] can be used to quantify the accuracy of a model's predictive capacity. Using a finite number of samples, conformal inference can provide guarantees on the model accuracy irrespective of the data distribution, or the method of model learning. [13] [2] explains such a method for model conformance.

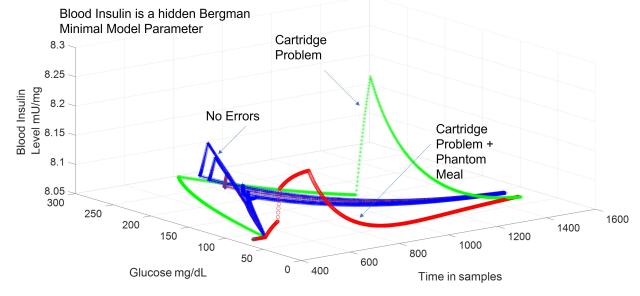


Fig. 5. Trajectories for no error, unknown error, and combination of known and unknown error are shown. Clearly, the trajectories are very different when internal PGSM model variables are considered. The cartridge problem trajectory on glucose would have satisfied STL defined on the output. None of the error trajectories satisfy STL on model coefficients.

#### VI. ARTIFICIAL PANCREAS EXAMPLE

For the AP example, the input set  $\Theta$  consists of insulin bolus and meal intake. The set  $\Theta$  was constructed by varying bolus value from 0 to 40 U while the meal intake was varied from 0 grams to 28 grams. The model  $M(\theta)$  for the AP was the T1D simulator, which is an FDA-approved simulator and widely used for evaluating AP controllers [14]. The subset of  $\theta \in \Theta$  used as sample traces that have no unknown errors given by the following vector:

$$\{Bolus, Meal\} = \{(12, 17), (28, 20), (7, 6), (14, 13), (17, 14), (32, 27), (15, 17), (20, 20), (10, 12), (12, 14), (25, 22), (5, 12)\} \quad (9)$$

The PGSM is the BMM discussed in Section I-2 with parameter set  $\omega$  as shown in Table II. The robustness of the STL  $\phi$  for model conformance checking is in Equation 10.

$$\rho(\phi, \omega) = \max_{i \in \{1 \dots 7\}} \text{abs}\left(\frac{\omega[i] - \omega_{sim}[i]}{\omega_{sim}[i]}\right) - 0.01, \quad (10)$$

where  $\omega_{sim}$  is the T1D simulator settings. We partition the input space  $\{Bolus, Meal\}$  into test  $I_2 = \{(12, 17), (28, 20), (7, 6), (14, 13), (17, 14), (32, 27)\}$  and train set  $I_1 = \{(15, 17), (20, 20), (10, 12), (12, 14), (25, 22), (5, 12)\}$ . The DiH-RNN in Section I-2 is used to obtain the parameters  $\omega$  for the train set as shown in Table I. The residue for each element in the test set is also shown there. Given a probability threshold  $1 - \alpha = 0.95$  we obtain  $d$  to be at position  $\lceil (6/2 + 1) * 0.95 \rceil = 4$ , i.e.  $d = 0.0048$ . The interval for the robustness value is  $[-0.0216, 0.0376]$ . Table I shows that for the insulin cartridge problem, the model conformance results show that the robustness values under various input configurations are falling outside the range. Hence, these scenarios are deemed to be non-conformal to the original model. A look at the trajectory will show that although the glucose level did not cross the STL-specified thresholds trajectories with unknown and known errors were very different from the trajectory for no error as shown in Fig. 5 in terms of the hidden model variables. As such these output trajectories will all satisfy the STL if it was evaluated on the output. However, since we evaluate the STL robustness on the PGSM coefficients, we can detect the change.

TABLE I  
PHYSICAL MODEL COEFFICIENTS DERIVED USING DIHRNN FOR TRAIN AND TEST SET.

Train / Test	$p_1$ 1/min	$p_2$ 1/min	$p_3 \frac{10^{-6}}{\mu U \cdot min^2}$	$p_4$	$n$ 1/min	$VoI$ dl	$G_b$ mg/dl	Residue
Simulation Settings	0.098	0.1406	0.028	0.05	199.6	-80	0.035	NA
Train	0.0978	0.1406	0.0262	0.0508	198.134	-80.64	0.0349	0
Test 1	0.0982	0.1405	0.0256	0.0530	198.1340	-80.2774	0.0329	0.0225
2	0.0979	0.1407	0.0274	0.0533	198.1340	-85.0589	0.0332	0.0028
3	0.0980	0.1405	0.0262	0.0528	198.1340	-85.0973	0.0348	0.0011
4	0.0981	0.1405	0.0267	0.0515	198.1340	-80.6921	0.0343	-0.0168
5	0.0979	0.1407	0.0273	0.0548	198.1340	-82.7676	0.0317	0.0328
6	0.0980	0.1404	0.0275	0.0534	198.1340	-82.3447	0.0328	0.0048

TABLE II  
COMPARISON OF PHYSICAL MODEL COEFFICIENTS DERIVED USING DIHRNN FOR DIFFERENT INSULIN BLOCKAGES, D IN THE ROBUSTNESS COLUMN  
MEANS ERROR DETECTED AND ROBUSTNESS IS BEYOND [-0.0216, 0.0376]. INSULIN = 7.5 U, MEAL = 20 GRAMS.

Insulin Block Percent-age	Time until insulin release	$p_1$ 1/min	$p_2$ 1/min	$p_3 \frac{10^{-6}}{\mu U \cdot min^2}$	$p_4$	$n$ 1/min	$VoI$ dl	$G_b$ mg/dl	Robustness
20	150	0.065	0.018	0.033	0.098	0.1404	268.55	-51.46	0.37 (D)
40	120	0.053	0.018	0.034	0.098	0.1402	287.92	-68.32	0.3885 (D)
80	90	0.068	0.019	0.034	0.098	0.1401	235.25	-58.68	0.36 (D)
70	70	0.068	0.020	0.033	0.098	0.1400	216.14	-48.12	0.43 (D)
60	50	0.068	0.019	0.034	0.098	0.1405	180.48	-69.76	0.35 (D)
Phantom 20	150	0.098	0.1402	0.0194	0.058	155.89	-54.104	0.0269	0.32 (D)
Phantom 40	120	0.098	0.1402	0.0218	0.0579	307.06	-60.73	0.0339	0.5284 (D)
Phantom 80	90	0.098	0.1401	0.0217	0.0503	143.43	-64	0.0344	0.27 (D)
Phantom 70	70	0.098	0.139	0.0229	0.0655	169.20	-48.26	0.0348	0.48 (D)
Phantom 60	50	0.0983	0.1400	0.0187	0.0554	317.86	-55.12	0.0349	0.5825 (D)

## VII. CONCLUSIONS

In this paper, our technique monitors the physical system in the CPS and models its behavior using a physics-guided surrogate model. We propose a dynamic dynamic-induced hybrid RNN-based learning methodology to derive the model coefficients of the PGSM from both model behavior and operational characteristics. A deviation in the evaluation criteria for model conformance between CPS model coefficients and operational model coefficients results in the detection of operational changes. Through this technique, we can identify unknown unknowns whose effects are hidden in the inner parameters of the CPS with minimal effect on the outputs. Early detection of such faults using this technique can potentially prevent future fault combinations that can potentially have fatal consequences.

## REFERENCES

- [1] A. Banerjee, I. Lamrani, and S. K. Gupta. Faultex: explaining operational changes in terms of design variables in cps control code. In *2021 4th IEEE International Conference on Industrial Cyber-Physical Systems (ICPS)*, pages 485–490. IEEE, 2021.
- [2] A. Banerjee, A. Maity, S. K. Gupta, and I. Lamrani. Statistical conformance checking of aviation cyber-physical systems by mining physics guided models. In *2023 IEEE Aerospace Conference*, pages 1–8. IEEE, 2023.
- [3] S. Biewer, P. R. D’argenio, and H. Hermanns. Doping tests for cyber-physical systems. *ACM Trans. Model. Comput. Simul.*, 31(3), aug 2021.
- [4] C. Dawson, S. Gao, and C. Fan. Safe control with learned certificates: A survey of neural lyapunov, barrier, and contraction methods, 2022.
- [5] A. Donzé and O. Maler. Robust satisfaction of temporal logic over real-valued signals. In *International Conference on Formal Modeling and Analysis of Timed Systems*, pages 92–106. Springer, 2010.
- [6] G. E. Fainekos and G. J. Pappas. Robustness of temporal logic specifications for continuous-time signals. *Theoretical Computer Science*, 410(42):4262–4291, 2009.
- [7] FDA.gov. Medtronic recalls minimed insulin pumps for incorrect insulin dosing. <https://www.fda.gov/medical-devices/medical-device-safety/medical-device-recalls>, 2021.
- [8] M. Krichen and S. Tripakis. Black-box conformance testing for real-time systems. In *International SPIN Workshop on Model Checking of Software*, pages 109–126. Springer, 2004.
- [9] I. Lamrani, A. Banerjee, and S. K. Gupta. Operational data-driven feedback for safety evaluation of agent-based cyber-physical systems. *IEEE Transactions on Industrial Informatics*, 17(5):3367–3378, 2020.
- [10] W. Li, D. Sadigh, S. S. Sastry, and S. A. Seshia. Synthesis for human-in-the-loop control systems. In E. Ábrahám and K. Havelund, editors, *Tools and Algorithms for the Construction and Analysis of Systems*, pages 470–484, Berlin, Heidelberg, 2014. Springer Berlin Heidelberg.
- [11] A. Maity, A. Banerjee, I. Lamrani, and S. K. Gupta. Cyphytest: Cyber physical interaction aware test case generation to identify operational changes. In *2022 IEEE 5th International Conference on Industrial Cyber-Physical Systems (ICPS)*, pages 01–06. IEEE, 2022.
- [12] National Highway Traffic Safety Association. Summary report: Standing general order on crash reporting for level 2 advanced driver assistance systems. *US Department of Transport*, June 2022.
- [13] X. Qin, Y. Xian, A. Zutshi, C. Fan, and J. V. Deshmukh. Statistical verification of cyber-physical systems using surrogate models and conformal inference. In *2022 ACM/IEEE 13th International Conference on Cyber-Physical Systems (ICCPs)*, pages 116–126. IEEE, 2022.
- [14] R. Visentin, E. Campos-Náñez, M. Schiavon, D. Lv, M. Vettoretti, M. Breton, B. P. Kovatchev, C. Dalla Man, and C. Cobelli. The uva/padova type 1 diabetes simulator goes from single meal to single day. *Journal of diabetes science and technology*, 12(2):273–281, 2018.
- [15] K. W. Weaver and I. B. Hirsch. The hybrid closed-loop system: evolution and practical applications. *Diabetes technology & therapeutics*, 20(S2):S2–16, 2018.
- [16] J. Yuan and Y. Weng. Physics interpretable shallow-deep neural networks for physical system identification with unobservability. In *2021 IEEE International Conference on Data Mining (ICDM)*, pages 847–856. IEEE, 2021.